International Journal of Mathematics Trends and Technology
ISSN: 2231-5373/ https://doi.org/10.14445/22315373/IJMTT-V68I7P512
Volume 68 Issue 7, 84-105, July 2022

Review Article

Effect of Buoyancy forces on Transient Airflow across Multiple Vents in Building with the Absence of Indirect Flow

Muhammad Auwal Lawan[1], Muftahu Zubairu Ringim[2], Lawan Adamu Isma'il[3]

[1,2,3]*Department of Mathematics, Kano University of Science and Technology, Wudil- Nigeria*

Received: 18 June 2022 Revised: 26 July 2022 Accepted: 31 July 2022 Published: 06 August 2022

Abstract - *The article is an extension of [15] work in which, the study investigatedthe effect of stack- driven airflow across multiple vents with the absence of indirect flow inthe building. Also, the study considered a building with multiple vertical openings which increased the exchange of air between the interior and exterior of the building envelope. This leads to the introduction of another dimensional group parameter (Grashop number Gr) in the study. Dimensional momentum and energy equations are utilized and solved analytically by means of separation of variable method. The behavior of parameters involved in the study predicted the results for Velocity, temperature distributions together with volumetric and mass- transfer. Moreover, the numerical simulations are presented graphically and discussed for varying values of physical parameters involved in the study.*

Keywords - *Airflow, Buoyancy forces, Multiple vents, Indirect flow.*

1. Introduction

Clearly, natural ventilation is not new. It is only in the past 200 years mechanical ventilation has been introduced. Prior to that period, all building envelopes occupied by humans were naturally ventilated. The first natural ventilation design can perhaps be considered as the time when these envelopes started to become purpose-building. Early designs were primarily empirical and evolved from experience. They might almost be described as long term experiments of full scale. In many countries, traditional passive cooling systems have developed alongside natural ventilation. Much of the experience gained over the centuries can be recognized in modern natural-ventilated buildings. A good example of this is the use of wind-assisted machines. However, modern buildings are more demanding of electricity and energy consumptions; Standards for health and comfort have to be met, while simultaneously satisfying requirements for low energy consumption and sustainability. Natural ventilation is process of supplying and removing air from an indoor space to the ambient by natural means. These can either caused by Wind- driven or Stack- driven effects.The advantages of natural ventilation in building is to save energy consumption, provide thermal comfort, removed air pollution and improve indoor air quality, with proper design appropriate to the building location and use, natural ventilation can replace all or part of a mechanical ventilation system. Both work on the principle of air moving from a high pressure to a low-pressure zone.Works have been carried out by many researchers in field of Fluid dymanics on Natural ventilation. [1] Performed an experimental investigation on scale effect in room airflow and then later [2] Studied Air movement on natural ventilated building. [3] Investigated the effect of Stack driven airflow across two openings. [4] Investigated the effect of indirect flow velocity in rectangular building across three verticalopenings. [5] Performed an experiment in a room airflow distribution system using computational fluid dynamic(CFD). [6] Studieda buoyancy-driven natural ventilation of buildings-impact of computational domain.[7] Considered the mixed ventilation when the interior of the building has uniform temperature. [8] Investigated displacement ventilation when the interior of the building was stratified. [9] Examined the effect buoyancy- driven forces of airflow on the floor of an enclosure in the presence of wind. [10] Developed a modelwith the effect of wind forces.[11] Examined the heat- transfer and airflow in interactive building façade. [12]Simulations were carried out to reproduce the decay of CO_2 concentration in a large semi-enclosed stadium. [13] Investigated natural convection flow for heat and mass- transfer in a single- sided ventilated building. [14] Considered ventilation potential model of airflow in china building. [15] Investigateda transient airflow across two verticalupper-vents in the absent of opposing flow in rectangular building. Experimentwere performed in heated, sealed room of a test house by [16]. [17] Investigated a vertical temperature distribution by combining natural and mechanical ventilation in an atrium building. [18] Iinvestigatedth effect of Stack- driven forces in single- sided ventilated building with large openings. [19] Investigated the effect of wind- driven flow in domain interacted with wind. [20] Investigated the effect of wind- driven flow in building with small openings. [21] Investigated the effect of two buoyancy forces on natural ventilation in an enclosure. [22] Studied natural

convection flow in a single- sided building with partition-I. [23] Studiednatural convection flow in a single sided building with partition-II. [24] Studied fluid mechanics of natural ventilation. [25] Investigated Stack- driven effectof airflow in cross-ventilated building with an opposing flow in one of the upper- vent. [26] Considered a Stack-driven air flow through multiple upper-vents in the presence of constant indirect flow velocity in Rectangular building. [27] A theoretical study on steady airflow in rectangular building in the presence of indirect flow was investigated. [28] A studied the effect of constant indirect flow velocity through multiple upper-vents in rectangular ventilated building using theoretical approach. [29] Studied natural convection flow in rectangular building with four openingsby stack- driven forces. [30] Studied airflow across vertical vents induced by stack- driven forces with an opposing flow in one of the upper openings.

The objectives of the researchis to investigate the effect of buoyancy forces on transient airflow across multiple vents in building with the absence of indirect flow.

The equations described the air flow are written in dimensionless form and solved by means of separation of variable approach. The effect of parameters involved in the research paper predicted the results of velocity profile, temperature profile together with volumetric airflow and mass- transfer.Lastly, the effect of changes of some selected values of parameters, such as Effective thermal coefficient (θ_0), Prandtl number(Pr),Grashof number(Gr) and discharge coefficient (c_d) were analyses and discussed in order find the one for optimal ventilation.

2. Building Discription

The building considered was the same as [15]. In which the building have multiple upper and one lowervertical openings. The upper openings maintained the area of $0.7m \times 1.0m$ each and the lower opening also maintained an area of $0.7m \times 2.0m$ with air as the connecting fluid which is illustrated in Fig. 1 and Fig. 2 below.

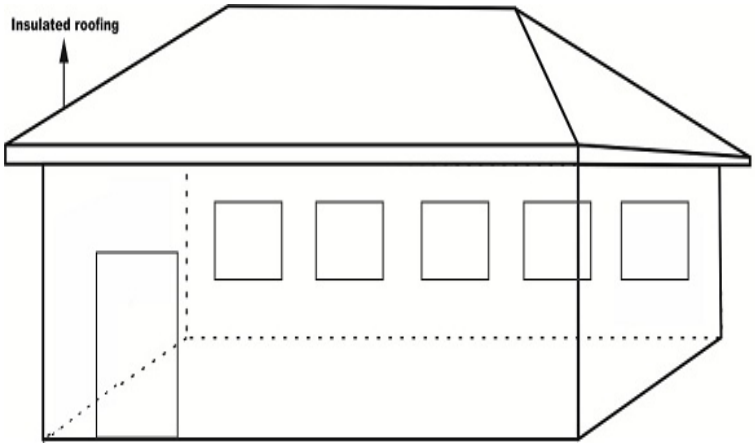

Fig. 1 Diagram of rectangular building with multiple upper vents.

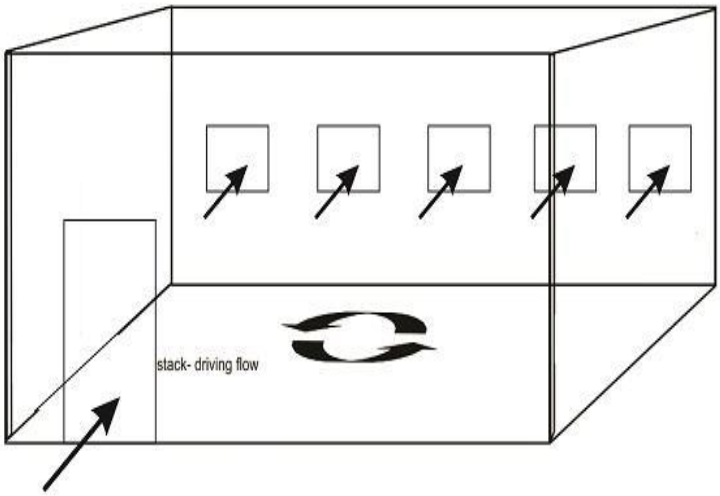

Fig. 2 Schematic diagram of airflow in rectangular building with multiple vents.

3. Problem Statement and Mathematical Formulation

The convective motion describing the problem is dimensional Momentum and Energy equations in which the continuity equation satisfied identically as,

$$\frac{\partial U}{\partial t} = g\beta\Delta\dot{\theta} + \nu\frac{\partial^2 U}{\partial y^2} \quad (1)$$

$$\frac{\partial \dot{\theta}}{\partial t} = \alpha\frac{\partial^2 \dot{\theta}}{\partial y^2}. \quad (2)$$

With the following dimensional boundary conditions as,

$0 \le y \le 2, t \ge 0, U(0) = 0,\ U(2) = 0, U(0,t) = 0,\ U(2,t) = 0,\ \dot{\theta}(0) = -\theta_0, \dot{\theta}(2) = 1 - \theta_0, \dot{\theta}(0,t) = 0, \dot{\theta}(2,t) = 0.$

By scaling height of the opening$y$ with y^*L, velocity U with$\frac{\nu U^*}{L}$, time t with$\frac{t^*L^2}{\alpha}$, and introducing temperature$\dot{\theta}$ with$\dot{\theta}^*\Delta\dot{\theta} + \theta_a$, where $\Delta\dot{\theta} = \dot{\theta} - \theta_a$.

In dimensionless form the above Equations (1) and (2) may be expressed as,

$$\frac{\partial U^*}{\partial t^*} = Pr\frac{\partial^2 U^*}{\partial y^{*2}} + PrGr\dot{\theta}^*(y^*, t^*)$$

$$\frac{\partial U^*}{\partial t^*} = Pr\frac{\partial^2 U^*}{\partial y^{*2}} + A\dot{\theta}^*(y^*, t^*) \quad (3)$$

$$\frac{\partial \dot{\theta}^*}{\partial t^*} = \frac{\partial^2 \dot{\theta}^*}{\partial y^{*2}} \quad (4)$$

Where, $A = PrGr$

with the following dimensionless boundary conditions as,

$0 \le y^* \le 1, t^* \ge 0, U^*(0) = 0, U^*(1) = 0, U_u^*(0,t^*) = 0,\ U_u^*(1,t^*) = 0, \frac{\partial U^*(1,t^*_{max})}{\partial y^*} = U_0,\ \dot{\theta}^*(0) = -\theta_0, \dot{\theta}^*(1) = 1 - \theta_0, \dot{\theta}_u^*(0,t^*) = 0, \dot{\theta}_u^*(1,t^*) = 0, \dot{\theta}_u^*(1,t^*_{max}) = Sint^*.$

Steady equation for (4) together with the boundary condition for dimensionless energy equation is,

$$\frac{d^2\dot{\theta}^*}{dy^{*2}} = 0 \quad (5)$$

$0 \le y^* \le 1, \dot{\theta}^*(0) = -\theta_0, \dot{\theta}^*(1) = 1 - \theta_0$

Yield the resulting solution for steady temperature as,

$$\dot{\theta}_s^*(y^*) = y^* - \theta_0 \quad (6)$$

The separation between the steady and unsteady part of solution are as follows,

$$\dot{\theta}^*(y^*, t^*) = \dot{\theta}_s^*(y^*) + \dot{\theta}_u^*(y^*, t^*) \quad (7)$$

The Equation (4) is also valid for the unsteady part of the solution as,

$$\frac{\partial \dot{\theta}_u^*}{\partial t^*} = \frac{\partial^2 \dot{\theta}_u^*}{\partial y^{*2}} \quad (8)$$

With the following boundary condition for dimensionless temperature profiles as,

$0 \le y^* \le 1, \dot{\theta}_u^*(0,t^*) = 0, \dot{\theta}_u^*(1,t^*) = 0, \dot{\theta}_u^*(1,t^*_{max}) = Sint^*.$

The separation given by,

$$\dot{\theta}_u^*(y^*, t^*) = Y(y^*)T(t^*) \quad (9)$$

Leads with Equation (8) to the eigen value problem as,

$$\frac{T'}{T} = \frac{Y''}{Y} + \frac{CY'}{Y} = -P_1^2, \text{For } P_1^2 > 0 \quad (10)$$

With generalized solution of the form,

$$\dot{\theta}_u^*(y^*, t^*) = K_3 e^{-P_1^2 t^*} sinh P_1 y^* \tag{11}$$

Equation (11), together with the homogeneous dimensionless boundary conditions yields to,

$$\dot{\theta}_u^*(y^*, t^*) = K_3 e^{-n^2\pi^2 t^*} sinhn\pi y^* \tag{12}$$

Similarly, using$\dot{\theta}_u^*(1, t_{max}^*) = sint^*$, from Equation (12) one obtains,

$$K_3 = \frac{sint^* e^{-n^2\pi^2 t_{max}^*}}{sinn\pi} for\ t^* \geq 0, n = \frac{1}{2}, \frac{3}{2}, \frac{5}{2}, \ldots.$$

The resulting Equation (12) becomes,

$$\dot{\theta}_u^*(y^*, t^*) = \frac{sint^* e^{-n^2\pi^2 (t_{max}^* - t^*)}}{sinn\pi} sinhn\pi y^* \tag{13}$$

The general time dependent solution for dimensionless temperature profiles is,

$$\dot{\theta}^*(y^*, t^*) = y^* - \theta_0 + \frac{sint^* e^{-n^2\pi^2 (t_{max}^* - t^*)}}{sinn\pi} sinhn\pi y^* \tag{14}$$

Steady equation for (3) together with the boundary condition for dimensionless momentum equation is,

$$Pr \frac{d^2 U^*}{dy^{*2}} = -A\dot{\theta}^*(y^*) \tag{15}$$

$0 \leq y^* \leq 1, U^*(0) = 0, U^*(1) = 0.$

Plugging the Equation (6) in Equation (15) yields to,

$$Pr \frac{d^2 U^*}{dy^{*2}} = -A(y^* - \theta_0) \tag{16}$$

Starting with the homogeneous part of Equation (16), one obtained the complementary solution as,

$$U_c^*(y^*) = C_1 + C_2 y^* \tag{17}$$

By employing the variation of parameter methods, one can write the particular solution as,

$$U_P^*(y^*) = Gr\left(\frac{\theta_0 y^{*2}}{2} - \frac{y^{*3}}{6}\right) \tag{18}$$

The general solution is given by,

$$U_s^*(y^*) = C_1 + C_2 y^* + Gr\left(\frac{\theta_0 y^{*2}}{2} - \frac{y^{*3}}{6}\right) \tag{19}$$

The two constant which appear in Equation (19) can be determined by prescribing the boundary condition for the steady velocity field in Equation (5), thus obtaining,

$$U_s^*(y^*) = Gr\left(\frac{\theta_0 y^{*2}}{2} - \frac{y^{*3}}{6} - \left(\frac{3\theta_0 - 1}{6}\right) y^*\right). \tag{20}$$

Where$C_1 = 0, C_2 = -Gr\left(\frac{\theta_0}{2} - \frac{1}{6}\right)$ are the two arbitrary constant.

Plugging the Equation (14) in (3) yields to,

$$\frac{\partial U^*}{\partial t^*} = Pr \frac{\partial^2 U^*}{\partial y^{*2}} + A(y^* - \theta_0) + \frac{sint^* e^{-n^2\pi^2 (t_{max}^* - t^*)}}{sinn\pi} sinhn\pi y^* \tag{21}$$

The separation between the steady and unsteady part of solution are as follows,

$$U^*(y^*, t^*) = U_s^*(y^*) + U_u^*(y^*, t^*) \tag{22}$$

The Equation (21) is also valid for the unsteady part of the solution as,

$$\frac{\partial U_u^*}{\partial t^*} = Pr \frac{\partial^2 U_u^*}{\partial y^{*2}} + A(y^* - \theta_0) + \frac{sint^* e^{-n^2\pi^2 (t_{max}^* - t^*)}}{sinn\pi} sinhn\pi y^* \tag{23}$$

With the following boundary condition for velocity profiles as,
$0 \le y^* \le 1,\ U_u^*(0,t^*) = 0,\ U_u^*(1,t^*) = 0.$

Starting with the homogeneous part of Equation (23), one obtain
$$\frac{dU^*}{dt^*} - Pr\frac{d^2U^*}{dy^{*2}} = 0 \tag{24}$$

The separation is given by the complementary solution as,
$$U_c^*(y^*,t^*) = Y(y^*)T(t^*) \tag{25}$$

Leads with Equation (24) to the eigen value problem as,
$$\frac{T'}{PrT} = \frac{Y''}{Y} = -P_2^2 \text{ for} P_2 > 0 \tag{26}$$

The generalized complementary solution is of the form,
$$U_C^*(y^*,t^*) = e^{-P_2^2 t^*}(C_3 cosP_2 y^* + C_4 sinP_2 y^*) \tag{27}$$

The particular solution for Equation (21) is given by,
$$U_P^*(y^*,t^*) = A\left(y^*t^* - \frac{Pry^{*3}}{6} - \left(\theta_0 t^* - \frac{\theta_0 Pry^{*2}}{2}\right) + \frac{sint^* e^{-n^2\pi^2(t^*_{max}-t^*)}}{sinn\pi} sinn\pi y^*\left(t^* - n^2\pi^2(1-Pr)\right)\right) \tag{28}$$

The generalized solution of unsteady velocity profiles is of the form,
$U_u^*(y^*,t^*) = U_C^*(y^*,t^*) + U_P^*(y^*,t^*)$

This yield to,
$$U_u^*(y^*,t^*) = e^{-P_2^2 t^*}(C_3 cosP_2 y^* + C_4 sinP_2 y^*) + A\left(y^*t^* - \frac{Pry^{*3}}{6} - \left(\theta_0 t^* - \frac{\theta_0 Pry^{*2}}{2}\right) + \frac{sint^* e^{-n^2\pi^2(t^*_{max}-t^*)}}{sinn\pi} sinn\pi y^*\left(t^* - n^2\pi^2(1-Pr)\right)\right) \tag{29}$$

The two constant which appear in Equation (29) can be determined by prescribing the boundary condition for the velocity field in Equation (22), thus obtaining,
$$U^*(y^*,t^*) = Gr\left(\frac{\theta_0 y^{*2}}{2} - \frac{y^{*3}}{6} - \left(\frac{3\theta_0 - 1}{6}\right)y^*\right) + e^{-P_2^2 t^*}(C_3 cosP_2 y^* + C_4 sinP_2 y^*) + A\left(y^*t^* - \frac{Pry^{*3}}{6} - \left(\theta_0 t^* - \frac{\theta_0 Pry^{*2}}{2}\right) + \frac{sint^* e^{-n^2\pi^2(t^*_{max}-t^*)}}{sinn\pi} sinn\pi y^*\left(t^* - n^2\pi^2(1-Pr)\right)\right) \tag{30}$$

$$C_3 = \theta_0 t^* e^{P_2^2 t^*}, C_4 = \frac{e^{P_2^2 t^*}}{sinP_1}\left(-\theta_0 t^* coshP_2 - t^* + \frac{Pr}{6} - \left(\frac{Pr}{2} - t^*\right)\theta_0 - sint^* e^{-n^2\pi^2(t_{max}-t^*)}\left(t^* - n^2\pi^2(1-Pr)\right)\right)$$

Therefore, the general time dependent solution for dimensionless velocity profiles is given by,
$$U^*(y^*,t^*) = Gr\left(\frac{\theta_0 y^{*2}}{2} - \frac{y^{*3}}{6} - \left(\frac{3\theta_0 - 1}{6}\right)y^*\right) + \theta_0 t^* cosP_2 y^* + CsinhP_2 y^*\left(-B\theta_0 t^* - t^* + \frac{Pr}{6} - \left(\frac{Pr}{2} - t^*\right)\theta_0 - sint^* e^{-D(t_{max}-t^*)}(t^* - E)\right) + A\left(y^*t^* - \frac{Pry^{*3}}{6} - \theta_0 t^* + \frac{\theta_0 Pry^{*2}}{2} + Fsint^* e^{-D(t_{max}-t^*)} sinn\pi y^*(t^* - E)\right) \tag{31}$$

The volumetric airflow is defined in Equation (32) below,
$$Q^*(y^*,t^*) = A_T^* c_d \int_{s=0}^{s=\frac{y^*}{2}} U^*(s)dsdt^* \tag{32}$$

Putting Equation (31) in (32), one obtains

$$Q^*(y^*,t^*) = A_T^* c_d \int_{s=0}^{s=\frac{y^*}{2}} \left[Gr\left(\frac{\theta_0 s^{*2}}{2} - \frac{s^{*3}}{6} - \left(\frac{3\theta_0 - 1}{6}\right)s^*\right) + \theta_0 t^* cosP_2 s^* + CsinhP_2 s^* \left(-B\theta_0 t^* - t^* + \frac{Pr}{6} - \left(\frac{Pr}{2} - t^*\right)\theta_0 - sint^* e^{-D(t_{max}-t^*)}(t^* - E)\right) + A\left(s^* t^* - \frac{Pry^{*3}}{6} - \theta_0 t^* + \frac{\theta_0 Prs^{*2}}{2} + Fsint^* e^{-D(t_{max}-t^*)} sinn\pi s^*(t^* - E)\right)\right] dsdt^* \quad (33)$$

The results for Equation (33) yields to volumetric air flow as,

$$Q^*(y^*,t^*) = A_T^* c_d \left[\left(Gr\left(\frac{\theta_0}{48}y^{*3} - \frac{1}{384}y^{*4} - \frac{(3\theta_0 - 1)}{48}y^{*2}\right)\right)t^* + Gy^* t^{*2} + H\left(1 - B\frac{y^*}{2}\right)\left(-I\frac{t^{*2}}{2} + JPrt^* - N(K(t^* - E)(sint^* - Kcost^*) + 2Lcost^* - Msint^*)e^{-D(t_{max}-t^*)}\right) + A\left(\frac{y^{*2}t^{*2}}{16} - \frac{Pry^{*4}t^*}{384} + \frac{\theta_0 Pry^{*3}t^*}{48} - \frac{\theta_0 t^{*3}y^*}{4} + O\left(1 - cosn\pi\frac{y^*}{2}\right)\left(N(K(t^* - E)(sint^* - Kcost^*) + 2Lcost^* - Msint^*)e^{-D(t_{max}-t^*)}\right)\right)\right] \quad (34)$$

The mass transfer is given by Equation (35) below as,

$$m^*(y^*,t^*) = \rho_a Q^* \quad (35)$$

By plugging Equation (34) in (35), one obtains the mass transfer as,

$$m^*(y^*,t^*) = A_T^* c_d \rho_a \left[\left(Gr\left(\frac{\theta_0}{48}y^{*3} - \frac{1}{384}y^{*4} - \frac{(3\theta_0 - 1)}{48}y^{*2}\right)\right)t^* + Gy^* t^{*2} + H\left(1 - B\frac{y^*}{2}\right)\left(-I\frac{t^{*2}}{2} + JPrt^* - N(K(t^* - E)(sint^* - Kcost^*) + 2Lcost^* - Msint^*)e^{-D(t_{max}-t^*)}\right) + A\left(\frac{y^{*2}t^{*2}}{16} - \frac{Pry^{*4}t^*}{384} + \frac{\theta_0 Pry^{*3}t^*}{48} - \frac{\theta_0 t^{*3}y^*}{4} + O\left(1 - cosn\pi\frac{y^*}{2}\right)\left(N(K(t^* - E)(sint^* - Kcost^*) + 2Lcost^* - Msint^*)e^{-D(t_{max}-t^*)}\right)\right)\right] \quad (36)$$

4. Analyses and Discussion

The section discussed the main features of the results obtained in equations (14), (31), (34) and (36). The analyses of the results are plotted in Fig 5- 40. While, comparisons with previous results will be plotted in Fig 41- 43. This is done in order to see the effect of changes of parameters to the overall flow distributions,while keeping other operating conditions and parameters fixed, and ascertain the best one for optimal natural ventilation.

The increase of effective thermal coefficient (θ_0) at Fig. 5- 7 shows an increase in the temperature profiles across the openings. Therefore, the building will be thermally comfortable. Fig. 8- 10, it reveals that increasing the Prandtl number (Pr) increases the velocity profiles across the openings. The increase of effective thermal coefficient (θ_0) at Fig. 11- 13 shows an increase in the velocity profiles within the building envelope but converges at both end of the walls due to the homogeneous velocity boundary condition. Fig. 14- 16, it reveals that increasing the Grashof number (Gr) increases the velocity profiles across the openings. Fig. 17- 19, it reveals that increasing the effective thermal coefficient (θ_0) increases the volumetric air flow in the building envelope. The increase of Prandtl number (Pr) at Fig. 20- 22 shows an increase in the volumetric air flow. Fig. 23- 25, it reveals that increasing the Grashof number (Gr) increases the volumetric air flow. The increase of discharge coefficient (c_d) at Fig. 26- 28 shows an increase in the volumetric air flow. Fig. 29- 31, it reveals that increasing the effective thermal coefficient (θ_0) increases the mass transfer from the interior of the building. The increase of Prandtl number (Pr) at Fig. 32- 34 shows an increase in the mass transfer. Fig. 35- 37, it reveals that increasing the Grashof number (Gr) increases the mass transfer. Almost displays the same flow pattern as Fig. 38-40, where the increase in discharge coefficient (c_d) also increases the mass transfer.

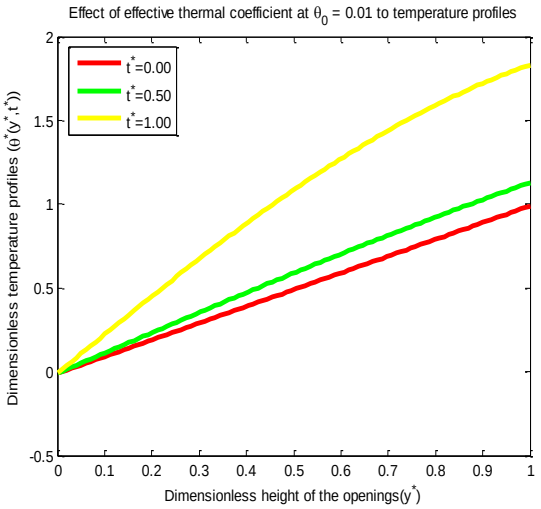

Fig. 5 Transient temperature profiles $\dot{\theta}^*$versusy^* and t^* for $\theta_0 = 0.01$

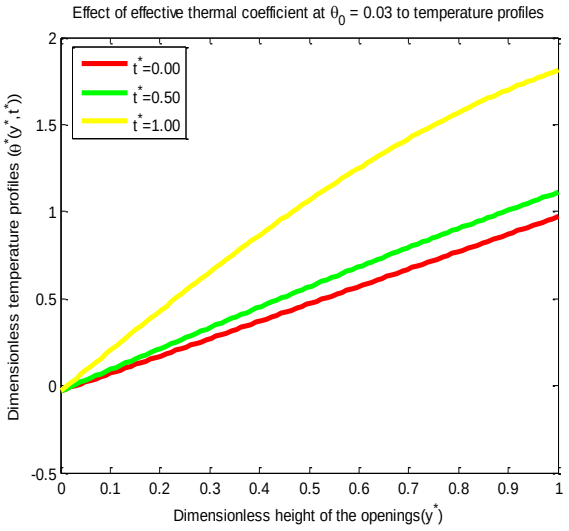

Fig 6. Transient temperature profiles $\dot{\theta}^*$versus y^* and t^* for $\theta_0 = 0.03$

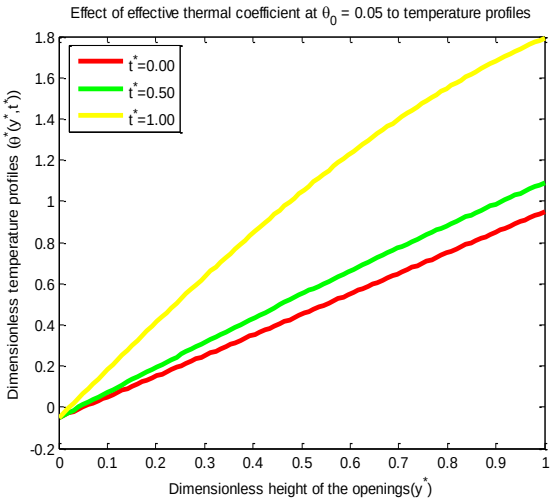

Fig. 7 Transient temperature profiles $\dot{\theta}^*$versusy^* and t^* for $\theta_0 = 0.05$

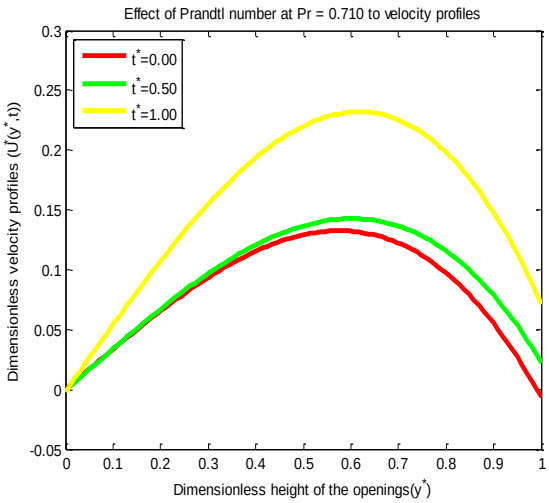

Fig. 8 Transient velocity profiles U^*versusy^* and t^* for $Pr = 0.710$ with fixed value of $\theta_0 = 0.03$ and $Gr = 1.5$

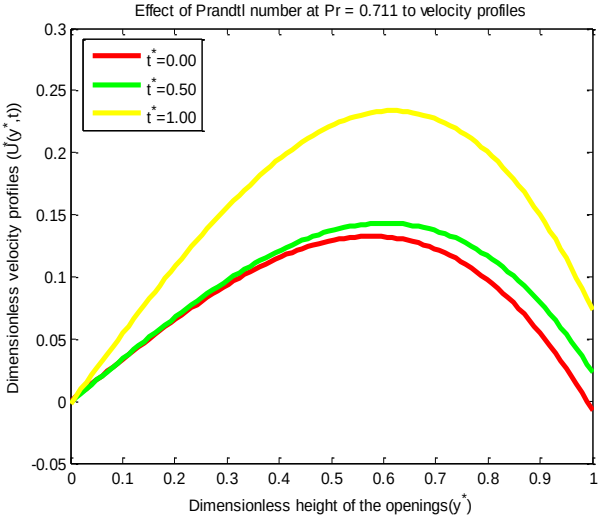

Fig. 9 Transient velocity profiles U^*versus y^* and t^* for $Pr = 0.711$ with fixed value of $\theta_0 = 0.03$ and $Gr = 1.5$

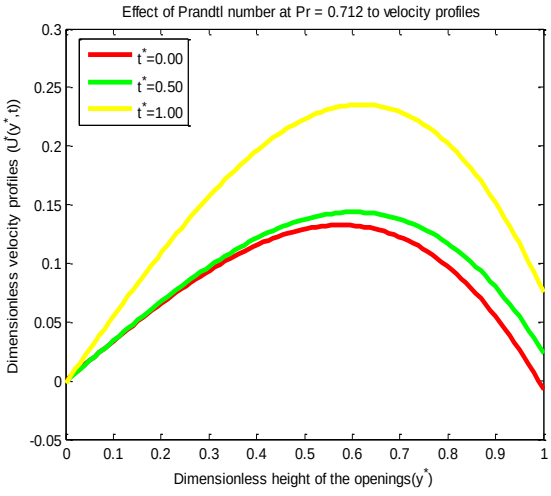

Fig. 10 Transient velocity profiles U^*versus y^* and t^* for $Pr = 0.712$ with fixed value of $\theta_0 = 0.03$ and $Gr = 1.5$

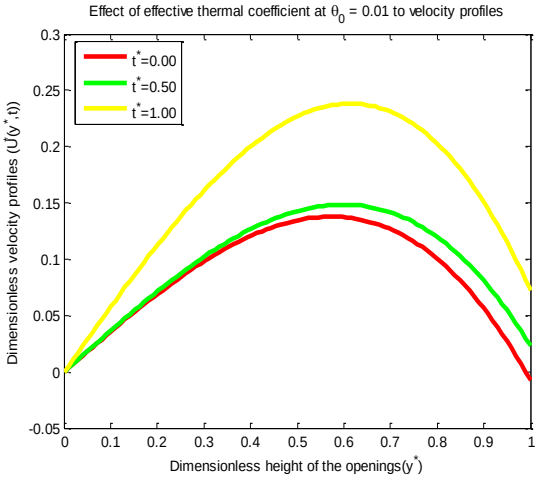

Fig. 11 Transient velocity profiles U^*versus y^* and t^* for $\theta_0 = 0.01$ with fixed value of $Pr = 0.710$and $Gr = 1.5$

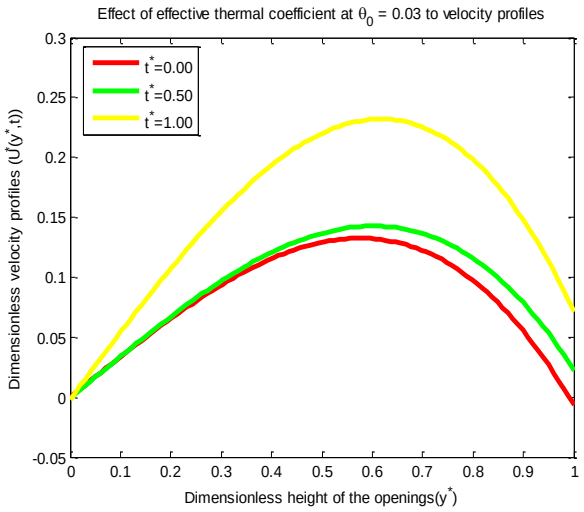

Fig. 12 Transient velocity profiles U^*versus y^* and t^* for $\theta_0 = 0.03$ with fixed value of $Pr = 0.710$and $Gr = 1.5$

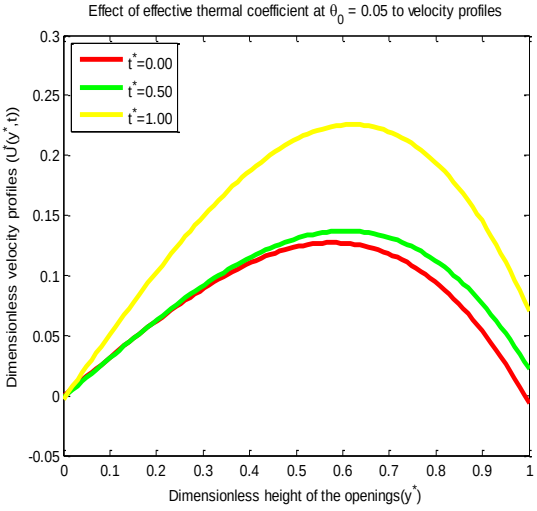

Fig. 13 Transient velocity profiles U^*versus y^* and t^* for $\theta_0 = 0.05$ with fixed value of $Pr = 0.710$and $Gr = 1.5$

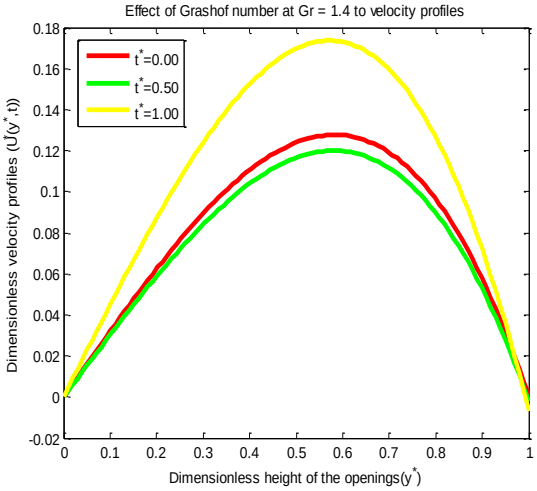

Fig. 14 Transient velocity profiles U^*versus y^* and t^* for$Gr = 1.4$ with fixed value of $\theta_0 = 0.03$ and $Pr = 0.710$

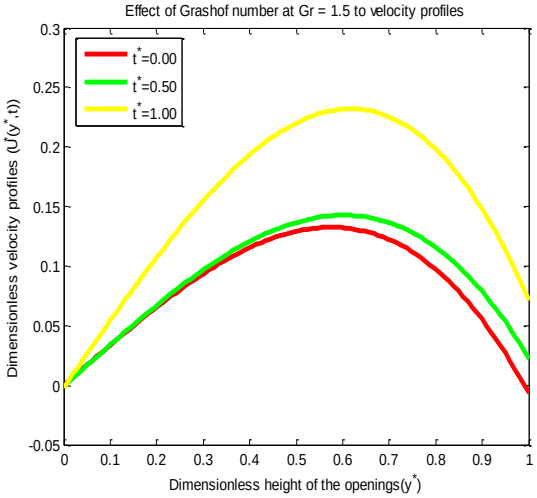

Fig. 15 Transient velocity profiles U^*versus y^* and t^* for$Gr = 1.5$ with fixed value of $\theta_0 = 0.03$ and $Pr = 0.710$

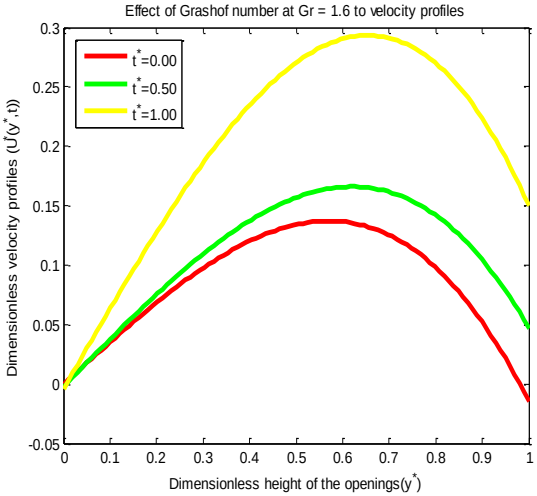

Fig. 16 Transient velocity profiles U^*versusy^* and t^* for$Gr = 1.6$ with fixed value of $\theta_0 = 0.03$ and $Pr = 0.710$

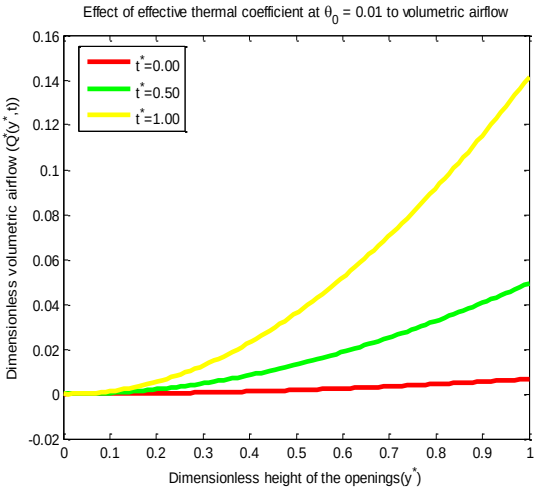

Fig. 17 Transient volumetric airflow Q^*versus y^* and $t^*$for $\theta_0 = 0.01$ with fixed value of $Pr = 0.710, C_d = 0.60$and $Gr = 1.5$

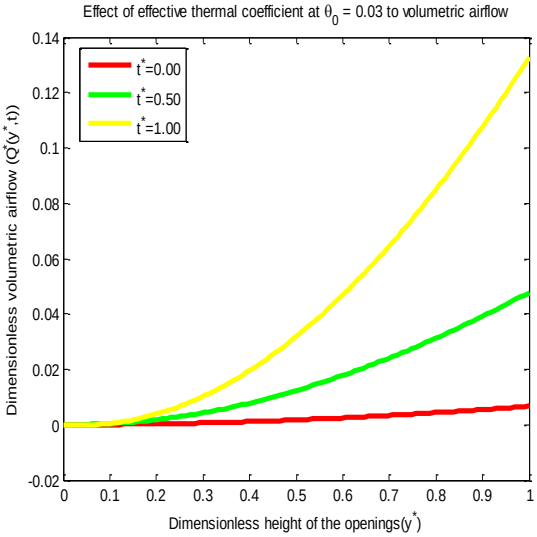

Fig. 18 Transient volumetric airflow Q^*versusy^* and t^* for $\theta_0 = 0.03$ with fixed value of $Pr = 0.710, C_d = 0.60$and $Gr = 1.5$

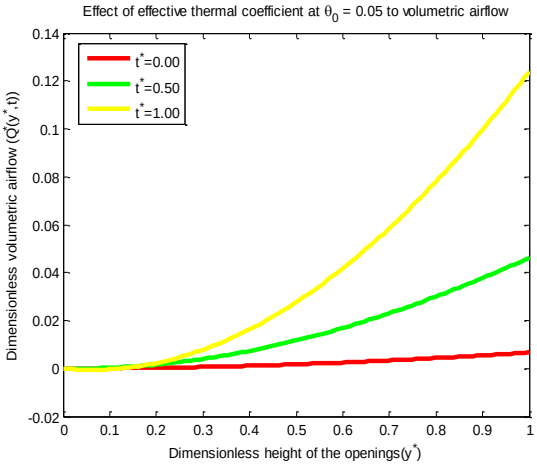

Fig. 19 Transient volumetric airflow Q^*versus y^* and t^* for $\theta_0 = 0.05$ with fixed value of $Pr = 0.710, C_d = 0.60$and $Gr = 1.5$

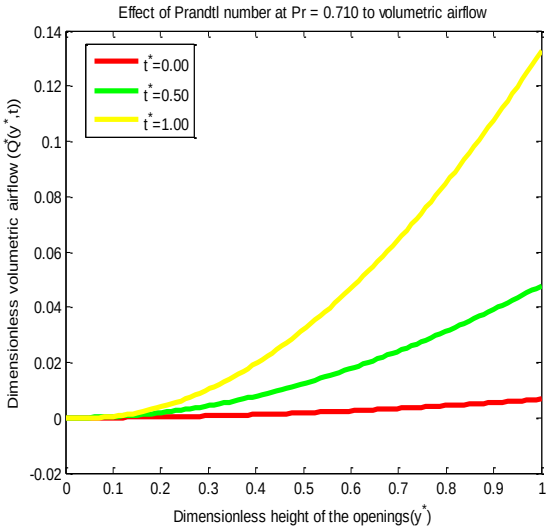

Fig. 20 Transient volumetric airflow Q^*versus y^* and t^* for $Pr = 0.710$ with fixed value of $\theta_0 = 0.03, C_d = 0.60$ and $Gr = 1.5$

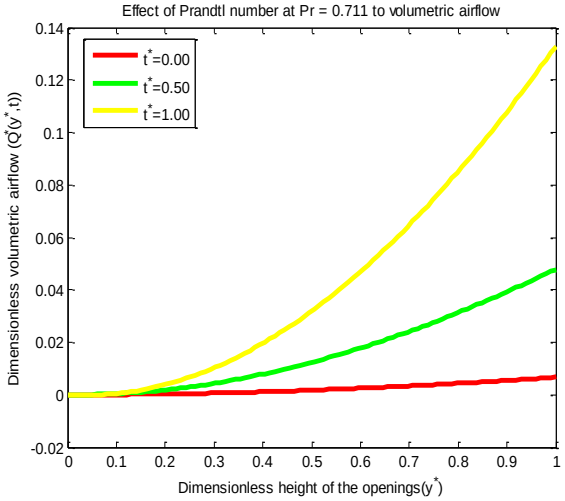

Fig. 21 Transient volumetric airflow Q^*versus y^* and t^* for $Pr = 0.711$ with fixed value of $\theta_0 = 0.03, C_d = 0.60$ and $Gr = 1.5$

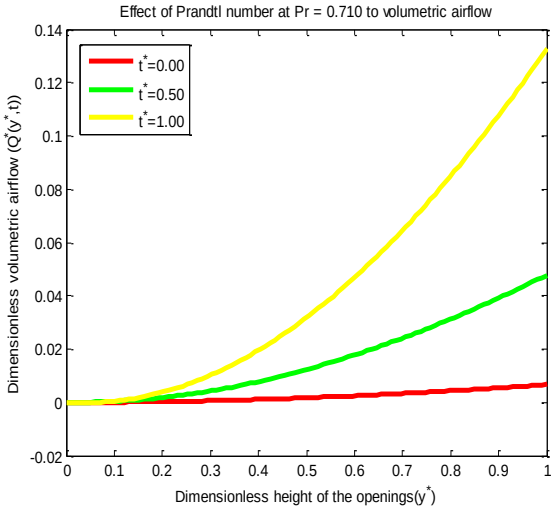

Fig. 22 Transient volumetric airflow Q^*versus y^* and t^* for $Pr = 0.712$ with fixed value of $\theta_0 = 0.03, C_d = 0.60$ and $Gr = 1.5$

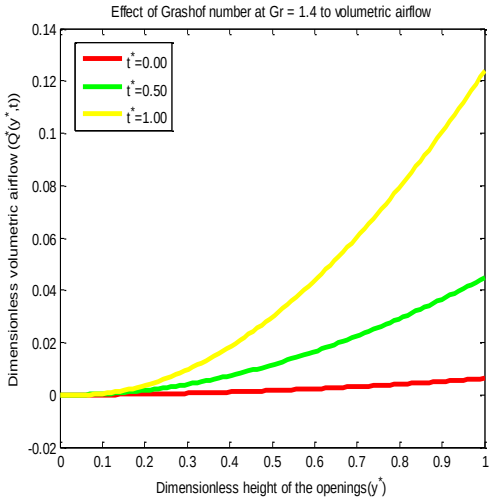

Fig. 23 Transient volumetric airflow Q^*versus y^* and t^* for $Gr = 1.4$ with fixed value of $\theta_0 = 0.03, C_d = 0.60$ and $Pr = 0.710$

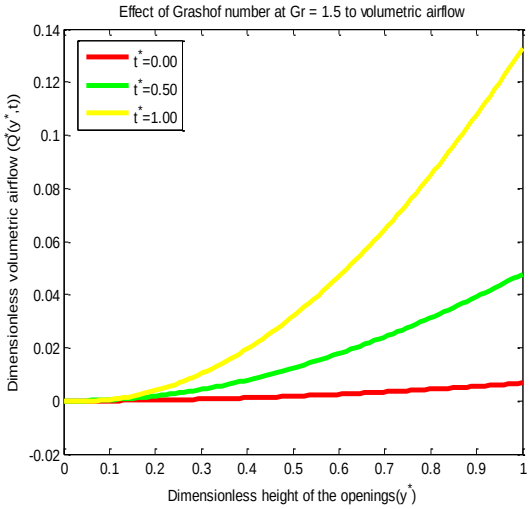

Fig. 24 Transient volumetric airflow Q^*versus y^* and t^* for $Gr = 1.5$ with fixed value of $\theta_0 = 0.03, C_d = 0.60$ and $Pr = 0.710$

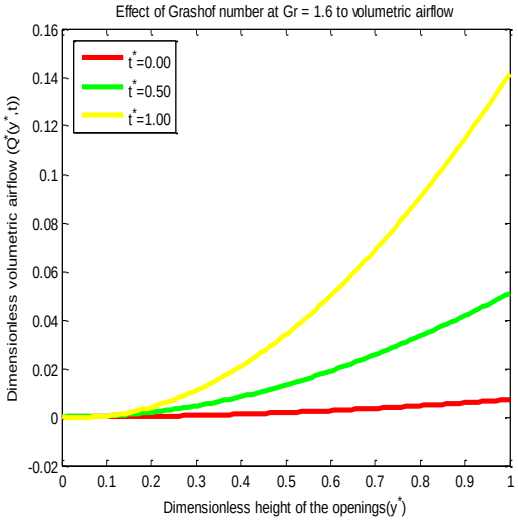

Fig. 25 Transient volumetric airflow Q^*versus y^* and t^* for $Gr = 1.6$ with fixed value of $\theta_0 = 0.03, C_d = 0.60$ and $Pr = 0.710$

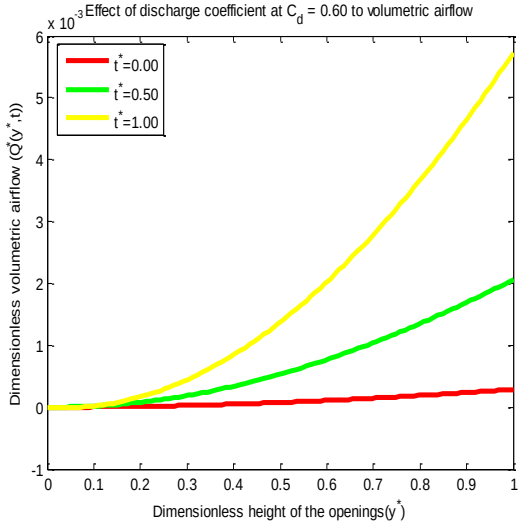

Fig. 26 Transient volumetric airflow Q^*versus y^* and t^* for $C_d = 0.60$ with fixed value of $\theta_0 = 0.03$, $Pr = 0.710$ and$Gr = 1.5$

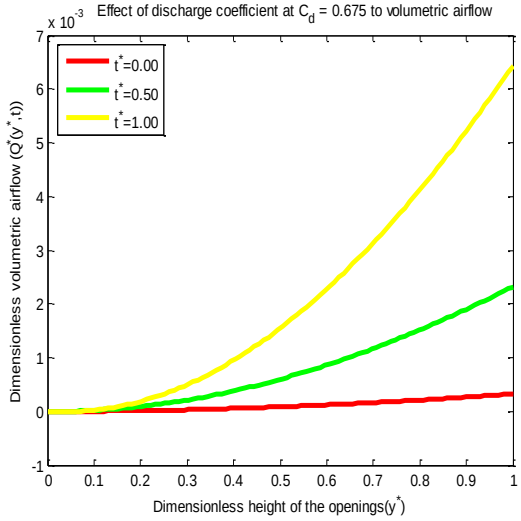

Fig. 27 Transient volumetric airflow Q^*versusy^* and t^* for $C_d = 0.675$ with fixed value of $\theta_0 = 0.03$, $Pr = 0.710$and$Gr = 1.5$

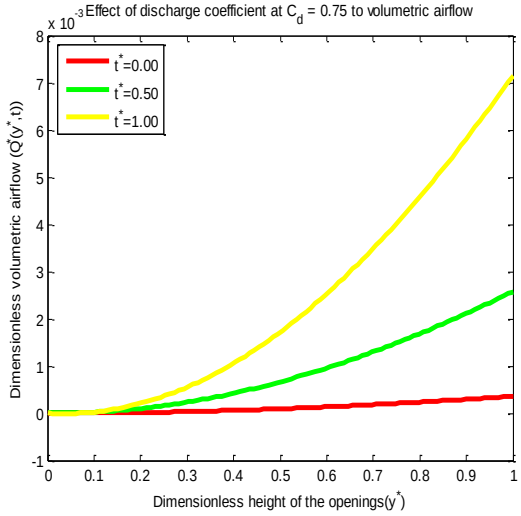

Fig. 28 Transient volumetric airflow Q^*versus y^* and t^* for $C_d = 0.75$ with fixed value of $\theta_0 = 0.03$, $Pr = 0.710$and$Gr = 1.5$

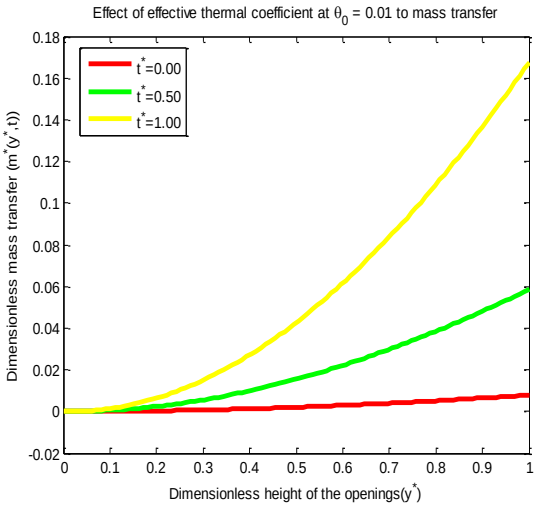

Fig. 29 Transient mass transfer m^*versus y^* and t^* for $\theta_0 = 0.01$ with fixed value of $Pr = 0.710, C_d = 0.60$ and $Gr = 1.5$

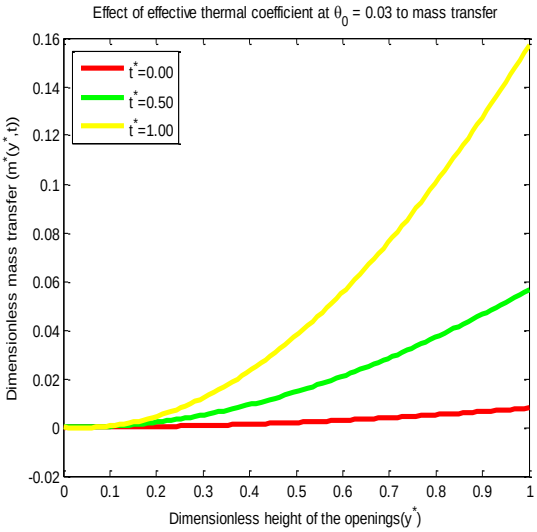

Fig. 30 Transient mass transfer m^*versus y^* and t^* for $\theta_0 = 0.03$ with fixed value of $Pr = 0.710, C_d = 0.60$ and $Gr = 1.5$

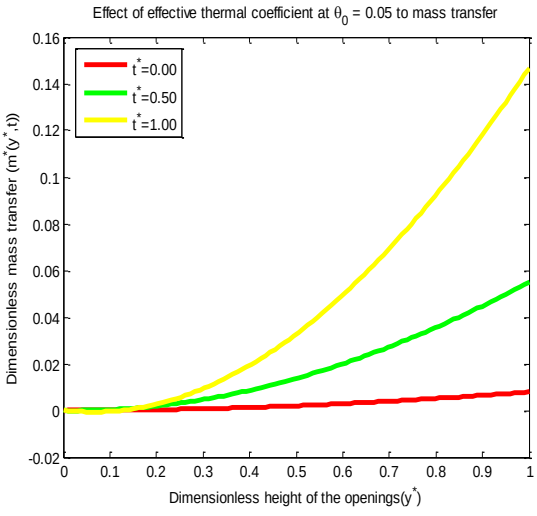

Fig. 31 Transient mass transfer m^*versus y^* and t^* for $\theta_0 = 0.05$ with fixed value of $Pr = 0.710, C_d = 0.60$ and $Gr = 1.5$

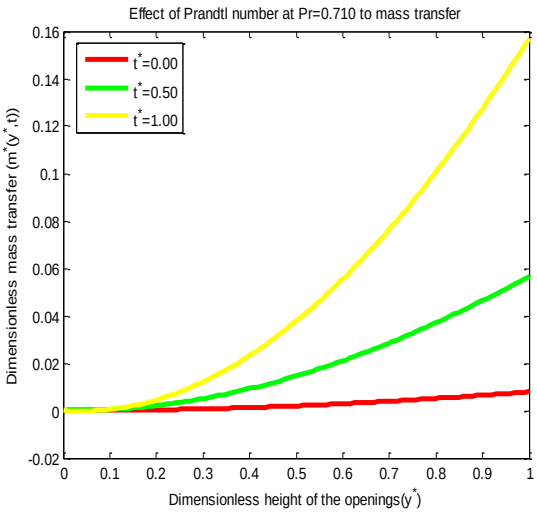

Fig. 32 Transient mass transfer m^*versus y^* and t^* for $Pr = 0.710$ with fixed value of $\theta_0 = 0.03. C_d = 0.60$ and $Gr = 1.5$

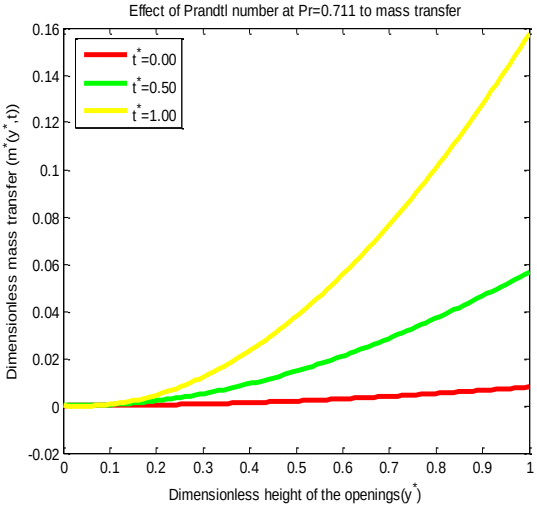

Fig. 33 Transient mass transfer m^*versus y^* and t^* for $Pr = 0.711$ with fixed value of $\theta_0 = 0.03, C_d = 0.60$ and $Gr = 1.5$

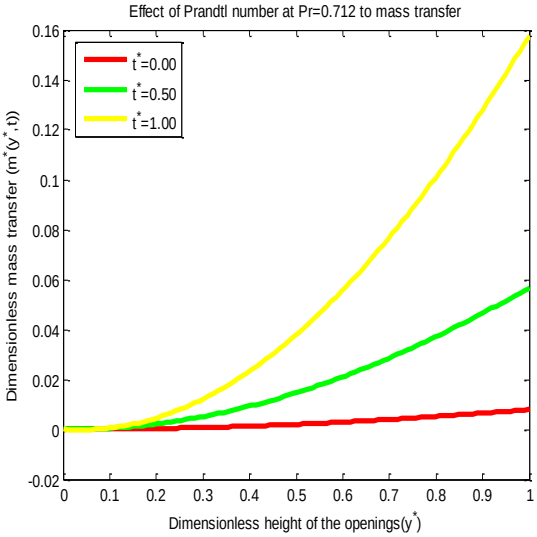

Fig. 34 Transient mass transfer m^*versus y^* and t^* for $Pr = 0.712$ with fixed value of $\theta_0 = 0.03, C_d = 0.60$ and $Gr = 1.5$

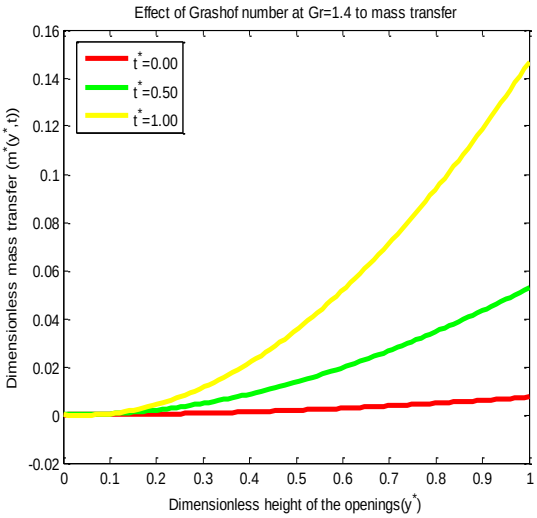

Fig. 35 Transient mass transfer m^*versusy^* and t^* for $Gr = 1.4$ with fixed value of $\theta_0 = 0.03, C_d = 0.60$ and $Pr = 0.710$

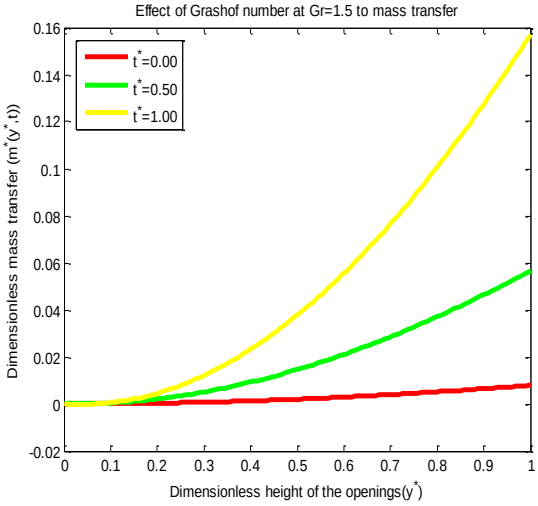

Fig. 36 Transient mass transfer m^*versus y^* and t^* for $Gr = 1.5$ with fixed value of $\theta_0 = 0.03, C_d = 0.60$ and $Pr = 0.710$

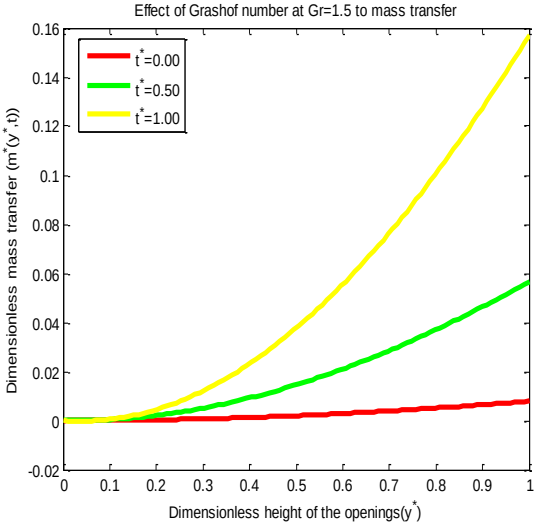

Fig. 37 Transient mass transfer m^*versus y^* and t^* for $Gr = 1.6$ with fixed value of $\theta_0 = 0.03, C_d = 0.60$ and $Pr = 0.710$

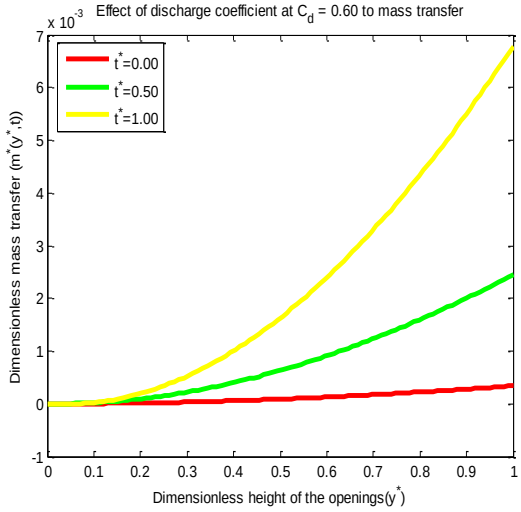

Fig. 38 Transient mass transfer m^* versus y^* and t^* for $C_d = 0.60$ with fixed value of $\theta_0 = 0.03$, $Pr = 0.710$ and $Gr = 1.5$

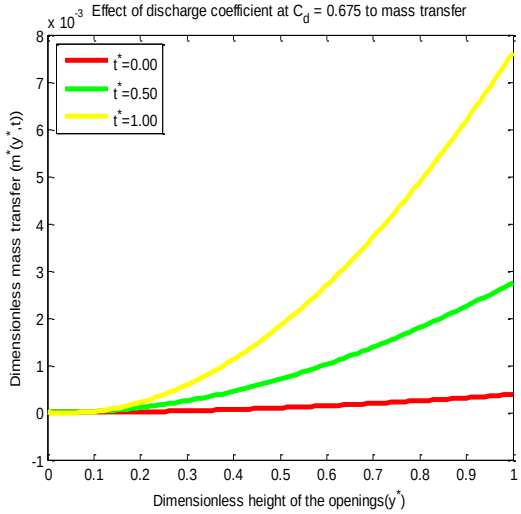

Fig. 39 Transient mass transfer m^* versus y^* and t^* for $C_d = 0.675$ with fixed value of $\theta_0 = 0.03$, $Pr = 0.710$ and $Gr = 1.5$

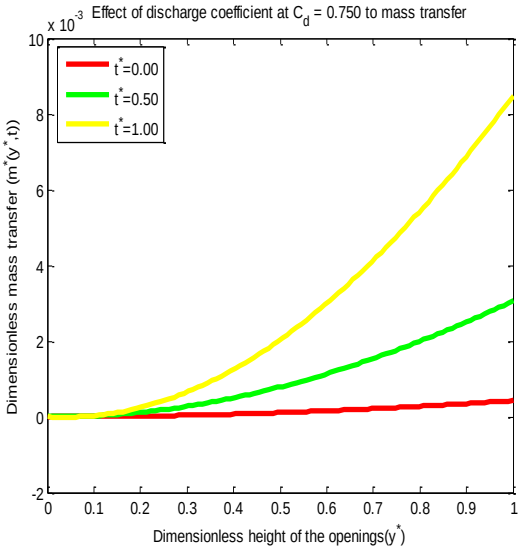

Fig. 40 Transient mass transfer m^* versus y^* and t^* for $C_d = 0.75$ with fixed value of $\theta_0 = 0.03$, $Pr = 0.710$ and $Gr = 1.5$

The results were compared with most closely related results given by [15] in Fig. 41- 43 below. It is worth mentioning that all the comparisons of the developed model are made in terms of non- dimensional variables are in good agreement with the previousintervation. And it is observed that, the best value for optimal natural ventilation is found to be in present developed study.

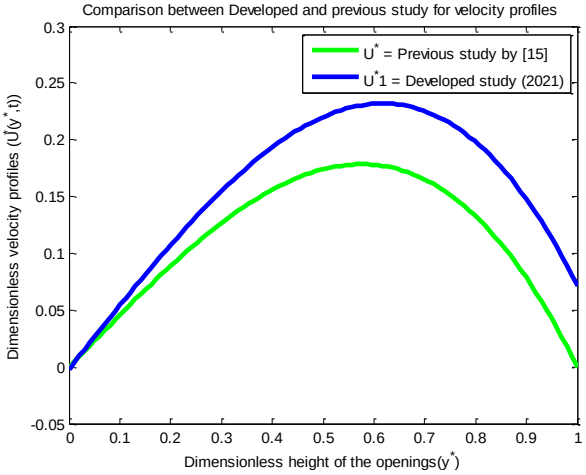

Fig. 41 Comparison betweenvelocity profiles $U^*$and U^*1 for fixed valueof $\theta_0 = 0.03, Pr = 0.710$, and $Gr = 1.5$

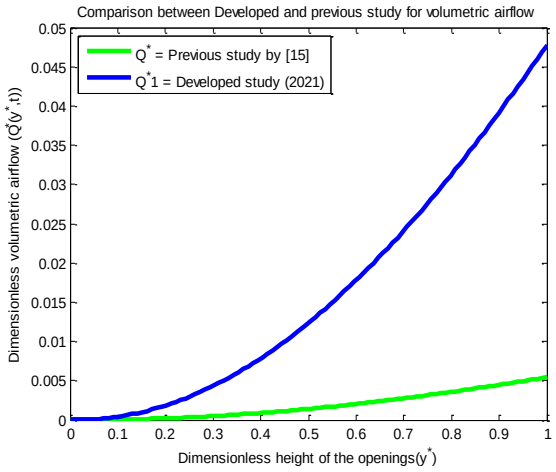

Fig. 42 Comparison between volumetric airflow Q^* and Q^*1 for fixed valuesof $\theta_0 = 0.03, C_d = 0.60, Pr = 0.710$, and $Gr = 1.5$

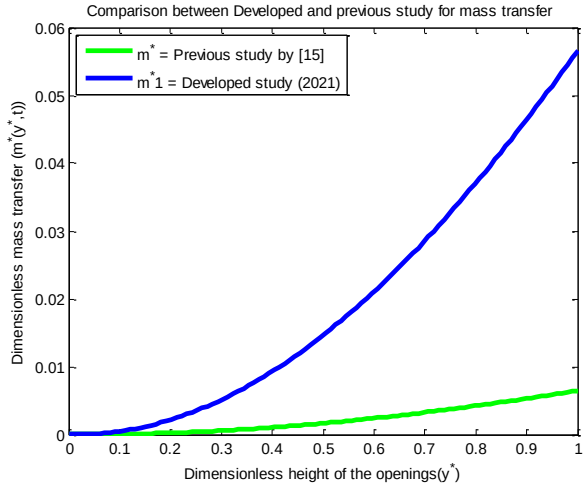

Fig. 43 Comparisonbetween mass transfer m^* and m^*1 for fixed valuesof $\theta_0 = 0.03, C_d = 0.60, Pr = 0.710$ and $Gr = 1.5$.

5. Conclusion

The paper studied the Transient effect Buoyancy forces across multiple vents in rectangular building with the absence of indirect flow. The governing equations describing the flow are written in dimensionless form and solved by means separation of variable approach. The effect of each physical parameter involved in the study are discussed with aid of plotted graphs.In order to examine the accuracy of our results, the results were compared with most closely related results given by [15]. It is worth mentioning that all the above comparisons of the developed model are made in terms of non- dimensional variables are in good agreement with the previousintervation. Hence, it is found that the best value for optimal natural ventilation is found to be in developed study. Therefore, expected objectives in the paper are achieved.

In conclusion, the following have been achieved.

1. Temperature profiles increases with an increasesof each parameters.
2. Velocity profiles across the openings increases with an increase of each parameters involved in the study.
3. Volumetric airflow increase with an increases of each parameters.
4. Mass- transfer increase with an increase of each parameters.

APPENDIX A

$$A_T^* = \frac{A_l A_{u1} A_{u2} A_{u3} A_{u4} A_{u5}}{\sqrt{A_l^2 + A_{u1}^2 + A_{u2}^2 + A_{u3}^2 + A_{u4}^2 + A_{u5}^2}}$$

$$A = PrGr$$

$$B = cosP_1$$

$$C = \frac{1}{sinP_1}$$

$$D = (n\pi)^2$$

$$E = (n\pi)^2(1 - Pr)$$

$$F = \frac{1}{sinn\pi}$$

$$G = \frac{sinP_1\theta_0}{4P_1}$$

$$H = \frac{1}{P_1 sinP_1}$$

$$I = \theta_0(1 + cosP_1) + 1$$

$$J = \frac{(1 - 3\theta_0)}{6}$$

$$K = \frac{1}{(n\pi)^2}$$

$$L = \frac{1}{(n\pi)^4\left(1 + \frac{1}{(n\pi)^4}\right)}$$

$$M = \frac{1}{(n\pi)^4}$$

$$N = \frac{1}{1 + \frac{1}{(n\pi)^2}}$$

$$O = \frac{1}{n\pi sinn\pi}$$

APPENDIX B

Nomencluture

A non- dimensional constant
C_1, C_2, C_3, C_4, K_3 coefficients
P_1, P_2 separation constant
$B, C, D, E, F, G, H, I, J, K, L, M, N, O$ arbitrary constants
A_T^* total area of the openings in non- dimensional Form
s dummy vaiable

P air pressure in dimensional form
g acceleration due to gravity
x_w constant width of the opening
y height of the opening in dimensional form
y^* height of the opening in non- dimensional form
t time in dimensional form
t^* time in non- dimensional form
c_d discharge coefficient
U_0 constant velocity of air at $y = 1, t = t_{max}$
U velocity of air in dimensional form
U^* velocity profile in non- dimensional form
U_s^* steady velocity profile in non- dimensional form
U_u^* unsteady velocity profile in non- dimensional form
U_c^* velocity profile in non- dimensional form for complementary solution
U_p^* velocity profile in non- dimensional form for particular solution

Greek Symbols

ρ_a ambient density of air
θ_a ambient temperature of air
θ_0 effective thermal coefficient
$\dot{\theta}$ air temperature in dimensional form
$\Delta\dot{\theta}$ change of air temperature in dimensional form
$\dot{\theta}^*$ temperature profile in non- dimensional form
$\dot{\theta}_s^*$ steady temp. profile in non- dimensional form
$\dot{\theta}_u^*$ unsteady temp. profile in non- dimensional form
β coefficient of thermal expansion
α thermal conductivity ratio
ν kinematic viscosity of fluid

Non Dimensional Groups

Pr Prandtl number
Gr Grashof number

Subscript

w width of the openings

Acknowledgment

The authors are grateful to authorities of Tertiary Education Trust Fund (TetFund), Nigeria and that of Kano University of Science and Technology, Wudil (KUST) for granting the leave and funds to conduct the research.

References

[1] H. B. Awbi and M. M. Nemri, "Scale Effect in Room Air-Flow Studies," *Energy and Buildings*, vol. 14, no. 3, pp. 207-210, 1990. Doi:10.1016/0378-7788(90)9044-J

[2] H. B. Awbi, "Air Movement on Naturally-Ventilated Buildings," *Renewable Energy*, vol. 8, no. 1, pp. 241-247, 1996. Doi:10.1016/0960-1481(96)88855-0

[3] A. L. Muhammad and A. B. Baffa and M. Z. Ringim, "Investigation of Stack- Driven Airflow through Rectangular Cross- Ventilated Building with Two Openings Using Analytic Technique," *International Journal of Computer Application (IJCA)*, vol. 141, no. 6, pp. 5-11, 2016. *Crossref*, https://www.ijcaonline.org/archives/volume141/number6/24786-2016909631

[4] A. L. Muhammad, D. A. Gano, M. Z. Ringim, S. A. Ibrahim and A.B. Baffa, "Theoretical Study on Steady Airflow Through Multiple Upper Openings Inside a Rectangular Building in the Presence of Indirect Flow," *Communication on applied Electronics (CAE)*, vol. 7, no. 14, pp. 17-25, 2018. *Crossref*, https://caeaccess.org/archives/volume7/number14/805-2018652757

[5] G. Gan, "Evaluation of Room Air Distribution Systems Using CFD," *Energy and Building*, vol. 23, no. 2, pp. 83-93, 1995.

[6] G. Gan, "Simulation of Buoyancy-Driven Natural Ventilation of Buildings-Impact of Computational Domain," *Energy and Building*, vol. 42, pp. 1290-1300, 2010.

[7] M. W. Liddament, "*A Review of Building Air Flow Simulation*," Tech. Note AIVC 33, Air Infiltration and Ventilation Centre, Coventry UK, 1991.

[8] S. Murakami and S. Kato, "Numerical and Experimental Study on Room Air Flow- 3-D Predictions Using the $K-E$ Turbulence Model," *Building and Environment*, vol. 24, no. 1, pp. 85-97, 1989.

[9] G. R. Hunt and P. F. Linden, "Steady-State Flows in an Enclosure Ventilated by Buoyancy Forces Assisted by Wind," *J. Fluid Mech*., vol. 426, pp. 355-386, 2001.

[10] D. N. Riahi, "*Mathematical Modeling of Wind Forces*," Department of Theoretical and Applied Mechanics, University of Illinois at Urbana- Champaign USA, pp. 1-14, 2005.

[11] F. Roberto, "Experimental and Numerical Analysis of Heat Transfer and Airflow on an Interactive Building Façade," *Energy and Buildings*, vol. 42, no. 1, pp. 23-28, 2010.

[12] T. Van Hooff, and B. Blocken, "CFD Evaluation of Natural Ventilation of Indoor Environments by the Concentration Decay Method: CO_2 Gas Dispersion from a Semi-Enclosed Stadium," *Building and Environment*, vol. 61, pp. 1-17, 2013.

[13] M. Santamouris, A. Argiriou, D. Asimakopoulos, N. Klitsikas and A. Dounis, "Heat and Mass- Transfer through Large Openings by Natural Convection," *Energy and Buildings*, vol. 23, pp. 1-8, 1995.

[14] Y. Wei, Z. Guoqiang, Y. Wei and W. Xiao, Natural ventilation potential model considering solution multiplicity, window opening percentage, air velocity and humidity in china, Building and Environment 45 (2010) 338- 344.

[15] A. L. Muhammad, M. Z. Ringim and L. A. Isma'il, Transient investigation of stack- driven airflow process through rectangular cross-ventilated building with two vents in the absence opposing flow in the upper opening, International Journal of Engineering and Technology (IJET) 7(3) (2018) 1249- 1256. https://www.sciencepubco.com/index.php/ijet/article/view/9422

[16] D. J. Wilson and D. E. Keil, Gravity-driven coun-terflow through an open door in a sealed room, Building and Environment 25 (1990) 379– 388.

[17] W. Xin, H. Chen and C. Weiwu, Mathematical modeling and experimental study on vertical temperature distribution of hybrid ventilation in an atrium building, Energy and Buildings 41 (2009) 907– 914.

[18] J. Yi and C. Qingyan, Buoyancy-driven single-sided natural ventilation in buildings with large openings, International Journal of Heat and Mass transfer 46 (2003) 973- 988.

[19] R. E. Britter, J. C. R. Hunt and J. C. Mumford, The distortion of turbulence by a circular cylinder, J. Fluid Mech. 92 (1979) 269- 301.

[20] L. C. James Lo, Predicting wind driven cross ventilation in buildings with small openings. Doctoral thesis. University of Texas, USA (2012).

[21] P. Cooper and P. F. Linden, Natural ventilation of an enclosure containing two buoyancy sources, J. Fluid mechanics 311 (1996) 153-176.

[22] W. G. Brown and K. R. Solvason, Natural convection through rectangular opening in partition-I. Int. J. Heat and Mass Transfer 5 (1962a) 859- 868.

[23] W. G. Brown and K. R. Solvason, Natural convection heat transfer through rectangular openings in partitions-II, Int. J. Heat and Mass Transfer 5 (1962b) 869 – 878.

[24] P. F. Linden, The Fluid Mechanics of Natural ventilation. Annu. Rev. Fluid Mech. 31(1) (1999) 201 - 238.

[25] A. L. Muhammad, A. B. Baffa and U. M. Dauda, Transient airflow process across three vertical vents induced by Stack- driven effect inside Un- Stratified cross- ventilated rectangular building with an opposing flow in one of the upper Opening, International Journal of Computer Application (IJCA) 148(1) (2016) 4- 11. https://www.ijcaonline.org/archives/volume148/number1/25719-2016910676

[26] Muhammad Auwal Lawan and Sunusi Aminu Nata'ala. Transient Investigation of Stack-Driven Air Flow Through Multiple Upper-Vents in The Presence of Constant Indirect Flow Velocity in Rectangular Ventilated Building. Engineering Mathematics 4(2) (2020), 14-30

[27] A. L. Muhammad et al. Theoretical study on steady airflow through multiple upper openings inside a rectangular building in the presence of indirect flow. Communications on Applied Electronics (CAE) 7(14) (2018), 17-25. http://dx.doi.org/10.19101/IJATEE.2020.762016

[28] Muhammad Auwal Lawan et al. A study of transient effect of constant indirect flow velocity through multiple upper-vents in un-stratified rectangular ventilated building using theoretical approach. International Journal of Advanced Technology and Engineering Exploration, 7(64) (2020), 53- 72

[29] Muhammad Auwal Lawan et al. A study of natural convection flow through rectangular building with four openings induced by stack-driven forces. International Journal of Mathematics Trends and Technology (IJMTT). 66(9) (2020), 228- 238. http://www.ijmttjournal.org

[30] A.L. Muhammad and A. B. Baffa. Air flow process across vertical vents induced by stack- driven effect with an opposing flow in one of the upper openings. International Journal of Computer Applications (IJCA), 123(1) (2015), 1-8. https://www.ijcaonline.org/archives/volume123/number1/21920-2015900728